The Journal of Experimental Biology 207, 4147-4155
Published by The Company of Biologists 2004
doi:10.1242/jeb.01239

The role of drag in insect hovering

Z. Jane Wang
Theoretical and Applied Mechanics, Cornell University, Ithaca, NY 14853, USA
e-mail: jane.wang@cornell.edu

Accepted 11 August 2004

Summary

Studies of insect flight have focused on aerodynamic lift, both in quasi-steady and unsteady regimes. This is partly influenced by the choice of hovering motions along a horizontal stroke plane, where aerodynamic drag makes no contribution to the vertical force. In contrast, some of the best hoverers – dragonflies and hoverflies – employ inclined stroke planes, where the drag in the down- and upstrokes does not cancel each other. Here, computation of an idealized dragonfly wing motion shows that a dragonfly uses drag to support about three quarters of its weight. This can explain an anomalous factor of four in previous estimates of dragonfly lift coefficients, where drag was assumed to be small.

To investigate force generation and energy cost of hovering flight using different combination of lift and drag, I study a family of wing motion parameterized by the inclined angle of the stroke plane. The lift-to-drag ratio is no longer a measure of efficiency, except in the case of horizontal stroke plane. In addition, because the flow is highly stalled, lift and drag are of comparable magnitude, and the aerodynamic efficiency is roughly the same up to an inclined angle about 60°, which curiously agrees with the angle observed in dragonfly flight.

Finally, the lessons from this special family of wing motion suggests a strategy for improving efficiency of normal hovering, and a unifying view of different wing motions employed by insects.

Key words: lift, drag, efficiency, dragonfly flight, normal hovering, unsteady aerodynamics

Introduction

Airplanes and helicopters are airborne *via* aerodynamic lift, not drag. However, it is not clear *a priori* that nature should design insects to fly using only lift. Historically, an insect wing has been viewed more often as an unsteady airfoil than a rowing oar. With such an analogy, studies of insect flight have focused on lift generation. This analogy with an unsteady airfoil would be appropriate if an insect wing moves at a relatively small effective angle of attack, in which case, lift, the force component orthogonal to the instantaneous velocity of the wing relative to the far field, is substantially greater than drag, the force component anti-parallel to the velocity. However, hovering insects tend to employ large angles of attack to generate high transient force, i.e. to take advantage of dynamic stall (Ellington, 1984; Dickinson and Götz, 1993; Dickinson, 1996; Ellington et al., 1996; Wang, 2000b). The typical angle of attack during hovering at 70% span is ~35–40°. At these angles, the lift and drag are of similar magnitude. Therefore, the separation of lift and drag in the classical sense is no longer appropriate.

Differentiating lift and drag may seem to be a matter of semantics. After all, living organisms presumably only care about the net forces. However, because theories of simple systems, such as an airfoil or a paddle, have influenced our approaches to understanding more complex locomotion in nature and our choices of model systems, in order to go beyond the confines of these theories it is necessary to first borrow the conventional terminology. Towards the end of this paper, we will see that this differentiation helps us to resolve one of the puzzles in quasi-steady estimates of dragonfly flight as well as to construct more efficient hovering strokes.

Viscous drag is often studied in the context of locomotion of microorganisms (bacteria, sperm and protozoa), which live in Stokes flow [Reynolds number (Re)=0; Purcell, 1977; Childress, 1981; Wu et al., 1975; Taylor, 1985]. The focus here is on the non-Stokesian regime. It was suggested that small insects might employ a drag mechanism at Re below ~100 (Horridge, 1956); however, use of drag is often found in large insects, such as butterflies, which use near vertical stroke plane at relatively higher Re (~10^3) (Ellington, 1984). The drag in these cases is dominated by pressure force. At even higher Re, some birds and fish also use pressure drag to fly and swim (Blake, 1981; Vogel, 1996). Thus, the Re, as long as it is sufficiently high to be outside the Stokesian regime, does not seem to determine whether an organism uses mainly drag or lift. Vogel (1996) reviewed the drag-based and lift-based thrust in aquatic motion. Using the example of a pedal motion parallel to the forward motion, i.e. rowing, he suggested that the '*drag-based system is better when the craft is stationary but lift-based system is superior at any decent forward speed*'. The motion considered by Vogel is appropriate for forward swimming and rowing but is different from typical hovering motions employed by insects. Recognizing that at high angle of attack

both lift and drag resulted from the same pressure force that acts normal to the wing, Dickinson (1996) suggested that '*the dichotomy between lift- and drag-based mechanisms of locomotion (Vogel, 1996) was blurred*'. Still, in subsequent studies, drag and lift have not been treated on equal footing. For example, most models approximated the stroke plane to be horizontal. While this is a reasonable simplification, it is also a special case where drag in two half-strokes is almost equal and in opposite direction, thus making negligible net contribution to the net force.

Some of the best hoverers – dragonflies and true hoverflies – employ asymmetric strokes along an inclined stroke plane, similar to rowing. This is in contrast to 'normal hovering' used by most insects including flies, bees and wasps, who flap their wings about a horizontal plane (Weis-Fogh, 1973). In normal hovering, a wing generates a vertical force in both half-strokes, while in asymmetric strokes it generates a vertical force primarily during the downstroke. This difference, together with the fact that normal hovering resembles a helicopter wing motion, prompted Weis-Fogh to hypothesize that normal hovering might be more efficient. This turns out not to be the case in the wing motions studied here, as I will show later.

A puzzle about hovering along an inclined stroke plane is that quick estimates of required lift coefficients based on blade-element theory, assuming constant lift and drag coefficient, range from 3.5 to 6 (Weis-Fogh, 1973; Norberg, 1975), which are substantially higher than those estimated for normal hovering insects: typically around 1 (see table 5 in Weis-Fogh, 1973). Later inclusion of corrections due to induced downward flow predicted similarly high coefficients (Ellington, 1984). Explaining these unusually large lift coefficients motivated a shift of focus from quasi-steady analysis to the investigation of unsteady mechanisms in hovering flight. Recently investigated mechanisms, such as dynamic stall (Dickinson and Götz, 1993; Ellington et al., 1996; Wang, 2000b), wing rotation and wing–wake interaction (Dickinson et al., 1999), can explain an increase of averaged lift up to a factor of two, but not a factor of four. This raises the question of whether the high coefficients seen in hovering with inclined stroke plane result from unsteady mechanisms alone or other assumptions made in the theoretical analyses.

Without getting into the details of the unsteady mechanisms, an obvious feature of a downward stroke along an inclined stroke plane is that the associated pressure drag has an upward vertical component, which can have a non-negligible contribution to weight balance. In the previous quasi-steady analyses, drag was assumed to be much smaller than lift. For example, the lift to drag ratio was assumed to be ~7 by Weis-Fogh (1973) and 6 by Norberg (1975). These were estimates based on the maximal value of lift to drag ratio from experiments on a locust wing (Jensen, 1956). Ellington (1984) used the relation $C_{D,pro} \approx 7/\sqrt{Re}$ based on flow past a cylinder and deduced a value of 0.15–0.2 at an Re of ~10^3 for the profile drag coefficient. While these values might be reasonable at a small angle of attack, they are considerable underestimates of drag at stalled angles during the downstroke.

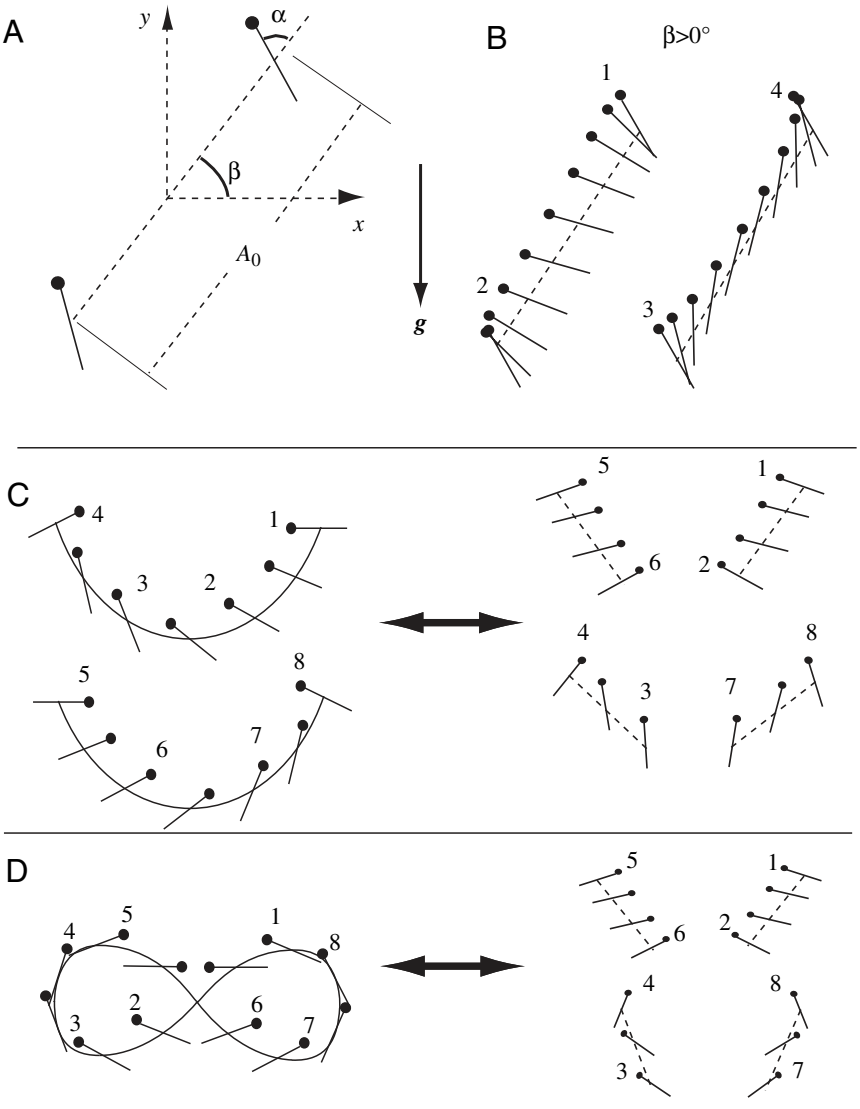

Fig. 1. Hovering motions studied in this paper. (A) The chord position (solid line with a black circle) and the coordinates, (B) generic asymmetric strokes along an inclined stroke plane, (C) normal hovering along a parabolic stroke plane and (D) normal hovering along a figure of eight. The strokes in C and D can be decomposed into pairs of asymmetric strokes described in B. The numbers next to the chords indicate the time sequence and also identify the corresponding segments in the decomposition.

Given that our ability to quantify unsteady forces, at least of model wings, is much improved, it seems worthwhile to re-examine the force generation and energy cost of hovering flight using different strategies. The first goal of this paper is to analyze these quantities in a family of hovering motions, which are parameterized by the inclined angle of the stroke plane and, correspondingly, different combinations of lift and drag in supporting the weight of an insect. The results offer an explanation of the discrepancy by a factor of four in the quasi-steady analysis. They also suggest a strategy for improving hovering efficiency and a unifying view of hovering motions used by different insects.

Models and methods

Wing motions

The trajectory of a rigid wing relative to a fixed body is described by three degrees of freedom, the position of a point on the wing in spherical coordinates (Θ, Φ) and the pitching angle (α) about the axis connecting the wing root and the point on the wing. The wing motions are thus specified by three periodic functions: $\Theta(t)$, $\Phi(t)$ and $\alpha(t)$. It is impractical to enumerate this family of kinematics by brute-force approach. The model chosen for this paper is one of the simplest possible family of a hovering motion but it allows us to study the dependence of forces and flow using different styles of hovering, similar to those seen in fruit flies or dragonflies.

In particular, I consider a two-dimensional cross-section of a wing executing the following motion:

$$[x(t), y(t)] = \frac{A_0}{2}(1 + \cos 2\pi ft)(\cos\beta, \sin\beta) \qquad (1)$$

$$\alpha(t) = \alpha_0 + B\sin(2\pi ft + \phi)\,, \qquad (2)$$

where $[x(t), y(t)]$ is the position of the center of the chord, $\alpha(t)$ is the chord orientation relative to the stroke plane, which is inclined at angle β (see Fig. 1A,B), f is the frequency, A_0 and B are the amplitudes of translation and rotation, respectively, and ϕ is the phase delay between rotation and translation. α_0 is the mean angle of attack and thus describes the asymmetry between the up- and downstrokes. $\alpha_0=\pi/2$ and $\beta=0$ correspond to a symmetric stroke along a horizontal plane. In other cases, for each α_0, β is determined such that the net force is vertically upward, corresponding to hovering.

Special cases of these wing motions have been studied theoretically (von Holst and Kuchemann, 1941), experimentally (Freymuth et al., 1991) and computationally (Gustafson et al., 1992; Wang, 2000a). Here I compute and extend the forces and flows for α_0 and β.

Computational methods

The flow around the wing is governed by the Navier–Stokes equation, which is solved with a fourth-order compact finite-difference scheme (E and Liu, 1996) in elliptic coordinates (Wang, 2000a,b; Wang et al., 2004).

The Navier–Stokes equation in the coordinates fixed to the wing has the form:

$$\frac{\partial \mathbf{u}}{\partial t} + (\mathbf{u}\cdot\nabla)\,\mathbf{u} = -\frac{\nabla p}{\rho} + \nu\Delta\mathbf{u} - d\mathbf{U}_0/dt - \left[\frac{d\boldsymbol{\Omega}}{dt}\times\mathbf{r} + 2\boldsymbol{\Omega}\times\mathbf{u} + \boldsymbol{\Omega}\times(\boldsymbol{\Omega}\times\mathbf{r})\right], \qquad (3)$$

$$\nabla\cdot\mathbf{u} = 0\,, \qquad (4)$$

$$\mathbf{u}\,|_{\text{wing}} = 0\,, \qquad (5)$$

where $\mathbf{u}$ is the velocity field, p is pressure, ν is kinematic viscosity, $\mathbf{r}$ is the position relative to the wing center and ρ is density. $\mathbf{U}_0$ and $\boldsymbol{\Omega}$ are the translational and rotational velocity of the wing, respectively. The last three terms correspond to the non-inertial force due to rotational acceleration, the Coriolis force and the centrifugal force, respectively. The Coriolis force and the centrifugal force disappear in the two-dimensional vorticity equation because they can be recast in terms of the gradient of a potential function. To ensure sufficient resolution at the edge of the wing and efficiency in computation, elliptic coordinates fixed to the wing (μ, θ) are employed and mapped to a Cartesian grid. The two-dimensional Navier–Stokes equation governing the vorticity in elliptic coordinates is:

$$\frac{\partial(S\omega)}{\partial t} + (\sqrt{S}\mathbf{u}\cdot\nabla)\omega = \frac{1}{Re}\nabla^2\omega\,, \qquad (6)$$

$$\nabla\cdot\sqrt{S}\mathbf{u}) = 0\,, \qquad (7)$$

where ω is the vorticity field, and S is the scaling factor $[S(\mu,\theta)=a^2(\cosh^2\mu-\cos^2\theta)]$, where a is a constant.

The velocity and vorticity are obtained in the non-inertial coordinates, which are then transformed into the inertial frame. The forces are calculated in the inertial frame by integrating the viscous stress along the wing:

$$\mathbf{F}_p = \rho\nu\int\frac{\partial\omega}{\partial\mathbf{r}}(y, -x)ds + \rho A_w\frac{d\mathbf{U}_0}{dt} \qquad (8)$$

$$\mathbf{F}_\nu = \rho\nu\int\omega\hat{s}ds\,, \qquad (9)$$

where $\mathbf{F}_p$ and $\mathbf{F}_\nu$ denote pressure and viscous forces, A_w is the cross-sectional area of the wing, s is arc length and $\hat{s}$ is the tangent vector along the ellipse, and the integral is over the contour of the ellipse. The instantaneous forces are non-dimensionalized by $0.5\rho U_{rms}^2 c$, where c is the chord. C_L and C_D denote the lift and drag coefficients normal and parallel to the relative flow field at infinity, and C_V and C_H are the vertical and horizontal force coefficients. Because the horizontal force cancels over a period, its absolute value is used when taking averages.

The translational motion of the wing is specified by two dimensionless parameters: the Reynolds number ($Re\equiv U_{max}c/\nu=\pi fA_0c/\nu$) and A_0/c. The typical Re of a dragonfly

is ~10^3, and that of a fruit fly is ~10^2. The *Re* dependence of the force was previously studied for similar wing motions from *Re*=15.7 to *Re*=1256 and it was shown that the averaged force does not have a strong dependence when 150<*Re*<1256 (Wang, 2000a), where the force is dominated by pressure (Wang et al., 2004). In the following computations, *Re*=150, A_0/c=2.5, *f*=1, *B*=π/4 and φ=0, which are in the range of observed values in insect hovering. These parameters are also where two-dimensional computations and three-dimensional experiments agree well (Wang et al., 2004).

Quasi-steady estimate

In addition to solving the Navier–Stokes equation, it was instructive to apply a quick quasi-steady estimate with a lift–drag polar obtained for a translating wing at *Re*=200 at an angle of attack (α_A) from [0,π] (Wang et al., 2004):

$$C_L = 1.2 \sin(2\alpha_A) , \quad (10)$$

$$C_D = 1.4 - \cos(2\alpha_A) . \quad (11)$$

For the sinusoidal motion studied here, the force due to coupling of pitching and translation averages zero, and the term due to wing acceleration is small by a factor proportional to the ratio of wing thickness to the stroke amplitude: thus, the estimates based on translational velocity are a reasonable approximation except near the wing reversal (Wang et al., 2004). See also Sane and Dickinson (2002) for inclusion of wing rotation. The results presented below are from two-dimensional computations, which contain the essential results from the quasi-steady analysis but also predict a non-trivial upper limit of the inclined angle of the stroke plane in this model.

Results

Two special cases: 'normal' hovering (α_0=90°, β=0°) vs *'dragonfly' hovering (α_0=60°, β=62.8°)*

I first contrast two special cases that have been studied most in the recent literature. The first case, where α_0=90° and β=0°, corresponds to a symmetric back and forth stroke along a horizontal plane. It is an idealization of normal hovering as seen, for example, in a fruit fly. The second case, where α_0=60° and β=62.8°, corresponds to hovering along an inclined stroke plane, similar to dragonfly wing motion.

Fig. 2 shows a side-by-side comparison of the wing motion, forces, vorticity field and mean flow in the two cases. In the case of a symmetric stroke (Fig. 2A), each half-stroke generates almost equal lift in the vertical direction and almost equal drag in the opposite horizontal direction. The averaged vertical and horizontal force coefficients are 1.07 and 1.61, respectively, resulting in a ratio of 0.66. By contrast, the asymmetric stroke (Fig. 2B) generates most of its vertical force during the downstroke, in which the lift and drag coefficients are 0.45 and 2.4, respectively; they are 0.50 and 0.68 during the upstroke. The vertical and horizontal force coefficients averaged over one period are 0.98 and 0.75, resulting in a ratio of 1.31, which is twice the value of the symmetric stroke. In this case, 76% of the vertical force is contributed by aerodynamic drag.

Comparing the vorticity field in the two cases shows a faster downward jet produced by the asymmetric stroke. Fig. 2Biv shows the time-averaged velocity below the wing. The velocity is plotted in physical space, which is interpreted from the computed velocity in the body coordinates. The symmetric stroke generates a jet whose width is comparable to the flapping amplitude, and it penetrates down for ~4–5 chords. By contrast, the asymmetric stroke generates a jet whose width is comparable to the chord, and it penetrates downward for ~7 chords. This difference may be significant when the wing is hovering above a surface, where the ground effect is non-negligible.

Ten cases from α_0=0 to α_0=90°

Next, I investigate how the flows, forces and specific power vary with the angle of the stroke plane (β). Fig. 3 shows the vorticity field of four representative cases in the fourth period. Ten snapshots are taken, equally spaced in time. The downward dipole jets are in the approximately opposite direction to the net force. The jet speed can be estimated by the travel distance over one period. It increases with β. At β=4°, 30°, 48°, 63° and 75°, the dipole pair travels over 2.4, 3, 3.5, 3.9 and 4 chords, respectively.

Fig. 4 shows the time-dependent vertical and horizontal forces for five cases. The averaged vertical forces are similar in all cases, as shown in Fig. 5. The fluctuation of the vertical force increases with β, while the fluctuation of the horizontal force decreases with β. For example, the maximum vertical force is approximately a factor of two higher at β=75° compared with β=4°, but the maximal horizontal force is approximately a factor of two lower. These variations are consistent with the fact that at larger β the downward jet is faster and narrower. The narrower jet at larger β makes sense since the wing sweeps less horizontal distance at a given A_0.

The variation of the force fluctuation may correlate with the body orientation during hovering. For an elongated body, it is preferable to hover with a horizontal body when employing a highly inclined stroke plane and with a vertical body when using a horizontal stroke plane (Weis-Fogh, 1973). Fig. 4 suggests that the body aligns in the direction where the force fluctuation is small, which would reduce body oscillations.

How do these different hovering styles affect the net forces and the specific power? Fig. 5 compares them as a function of β. It illustrates two interesting points. First, as the stroke plane tilts up, the average vertical force coefficient, $\bar{C}_V$, remains almost constant up to β≈60°. The horizontal force averages zero, but its average magnitude, $\bar{C}_H$, decreases with β. Thus, the ratio $\bar{C}_V/\bar{C}_H$ increases by a factor of two as β increases from 0° to 60°. Second, the averaged power exerted by the wing to the fluid is given by $\bar{P} = F_D(t)u(t)$, where $F_D(t)$ is the drag. Comparing this power with the ideal power based on the

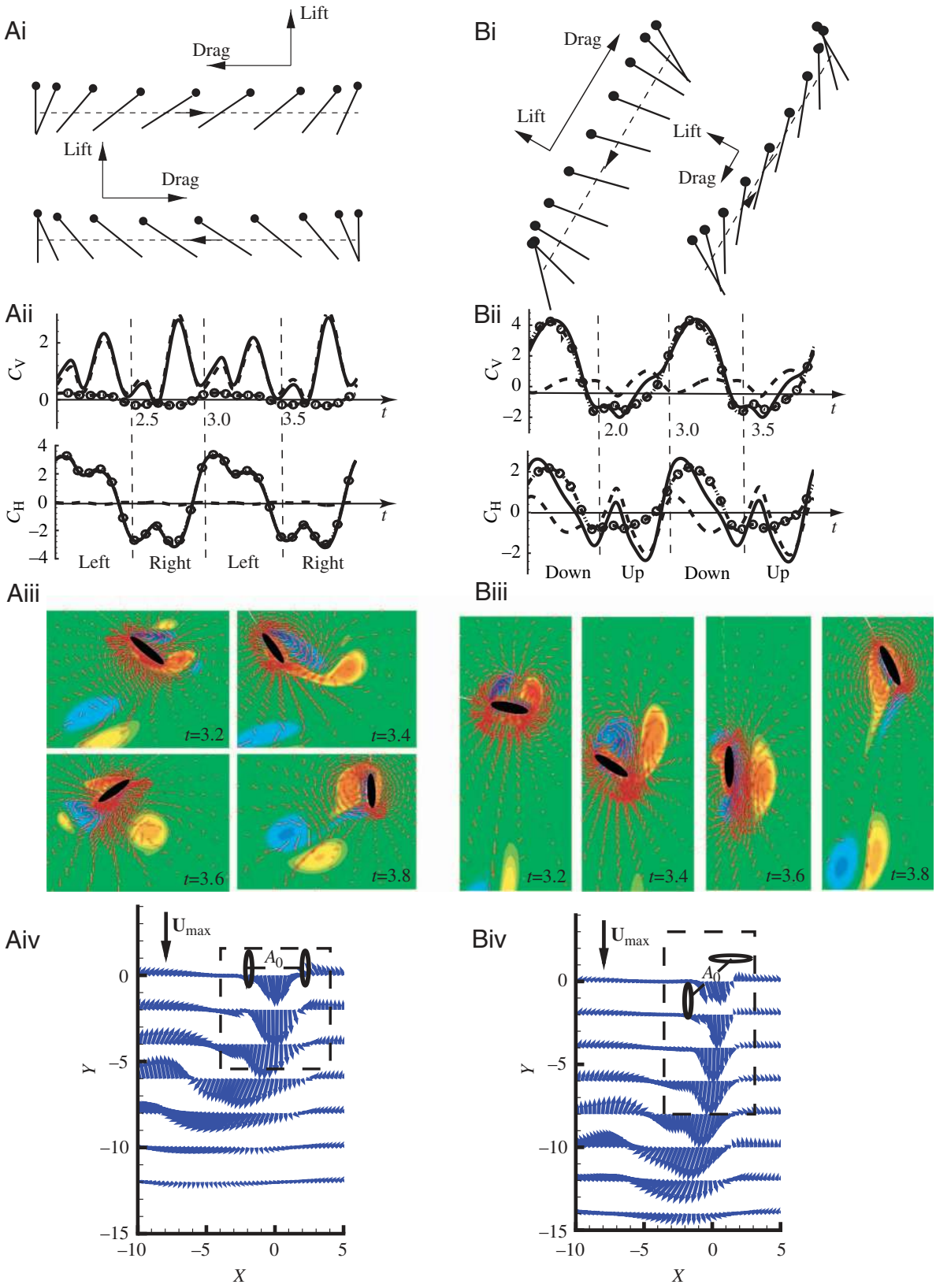

Fig. 2. Comparison of idealized normal hovering along a horizontal stroke plane (A) and dragonfly hovering along an inclined stroke plane (B). (i) Wing motion and averaged lift and drag, (ii) instantaneous vertical (C_V) and horizontal (C_H) force coefficients (solid line, net force; broken line, lift contribution; dotted line with circles, drag contribution), (iii) snapshots of vorticity (red, counterclockwise rotation; blue, clockwise rotation) and velocity fields (red vectors) during the fourth period, and (iv) time-averaged velocity field over one period (blue vectors). The maximum translational velocity ($\mathbf{U}_{max}$) serves as a reference velocity scale. The broken square corresponds to the region shown in iii.

actuator disk theory (Leishman, 2000) gives a non-dimensional measure:

$$\overline{C}_P = \frac{\langle F_D(t)u(t)\rangle}{\langle F_V(t)\rangle^{3/2}}\sqrt{2\rho A_0}\,, \tag{12}$$

where the size of the actuator for a two-dimensional wing is assumed to be the amplitude A_0, and F_V is the vertical force. Similar to $\overline{C}_V$, $\overline{C}_P$ is relatively independent of β up to β≈60°. Up to β=40°, there is a slight decrease in power required to balance a given weight. Although the ratio of the vertical to horizontal forces increases by a factor of 2 as β increases from 4° to 63°, the specific power is roughly the same. There is also a sharp decrease in vertical forces at β≈60°, which is not predicted by a quasi-steady model (Z.J.W., unpublished).

The mechanism for this cut-off requires further investigation, but it is worth noting that β≈60° agrees with one of the largest angles observed in free hovering flight of *Aeschna juncea* (Norberg, 1975); studies of tethered flight reported smaller inclined angles (Ellington, 1984; Wakeling and Ellington, 1997).

Discussion

While the above results are specific to the model chosen here, we can learn at least two general lessons. First, the force ratio (lift to drag ratio or vertical to horizontal force ratio) is no longer an appropriate measure of efficiency for hovering flight, except in the case of horizontal stroke plane. The examples seen here show that the specific power ($\overline{C}_P$) remains roughly constant while the force ratio ($\overline{C}_V/\overline{C}_H$) varies by about a factor of two. Second, hovering along an inclined stroke plane can be as efficient as normal hovering.

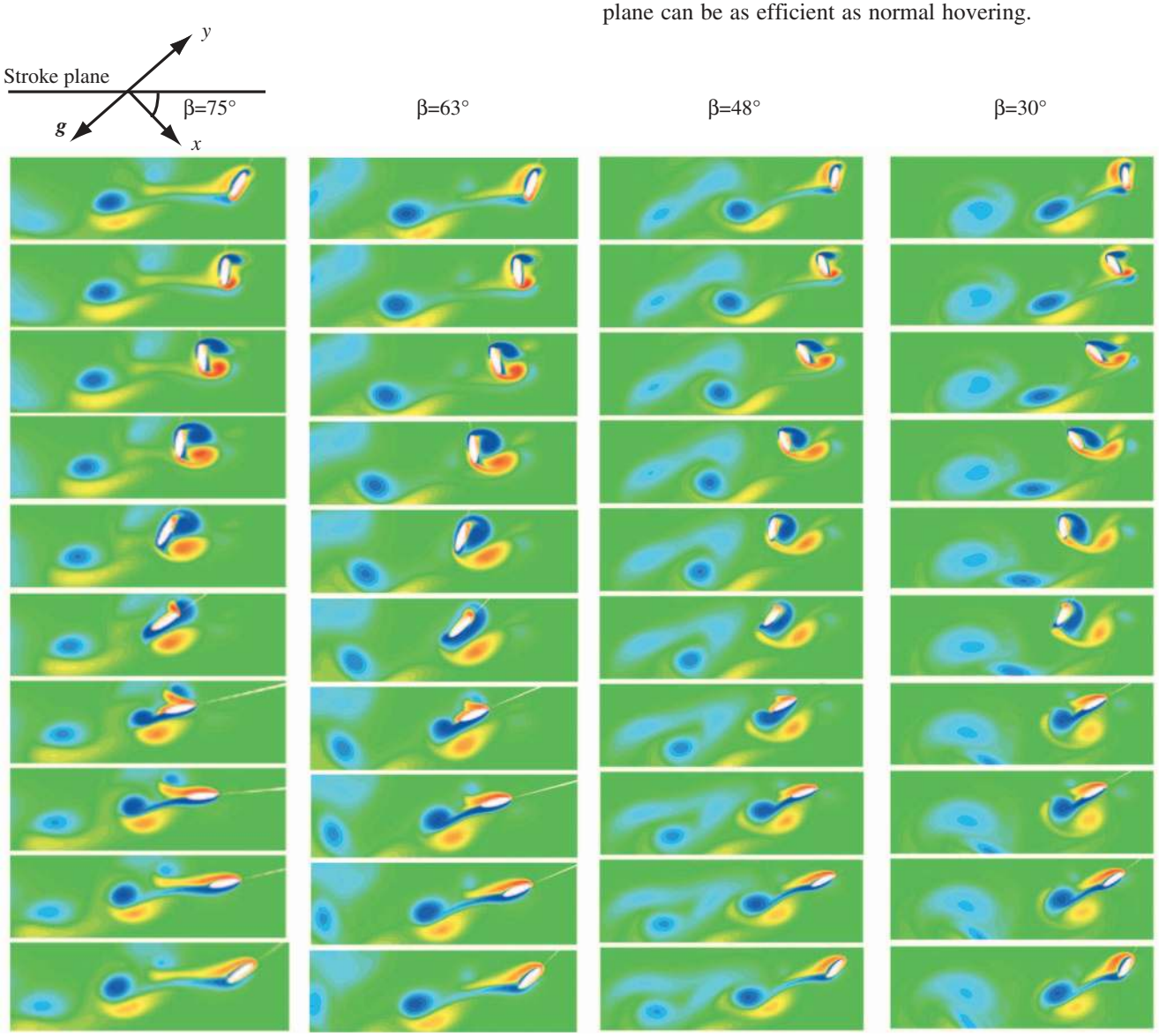

Fig. 3. Vorticity field in four cases, β=75°, 63°, 48° and 30°. In each case, 10 snapshots equally spaced over one period are shown (red, counterclockwise rotation; blue, clockwise rotation). The elliptic wing is in white. The stroke plane is horizontal for graphing purposes. The direction of gravity (***g***) relative the stroke plane is shown at the top left.

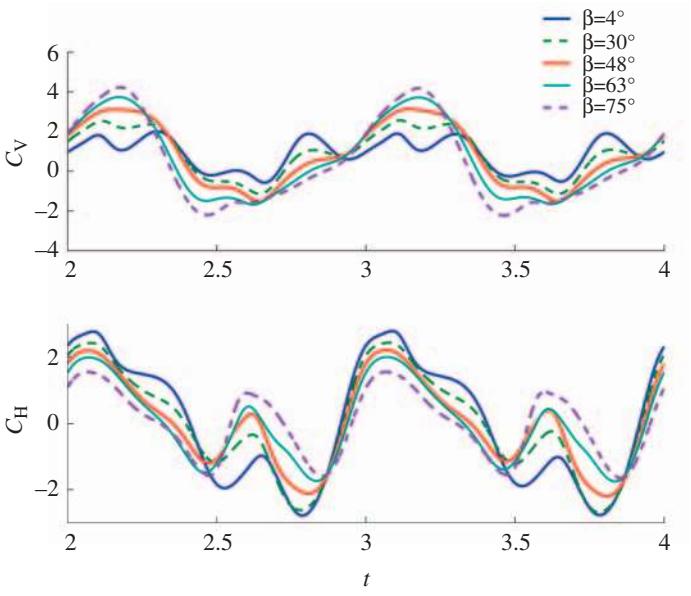

Fig. 4. Instantaneous vertical (C_V) and horizontal (C_H) force coefficients in the cases of β=75°, 63°, 48°, 30° and 4°. *t* is dimensionless (normalized by the flapping period).

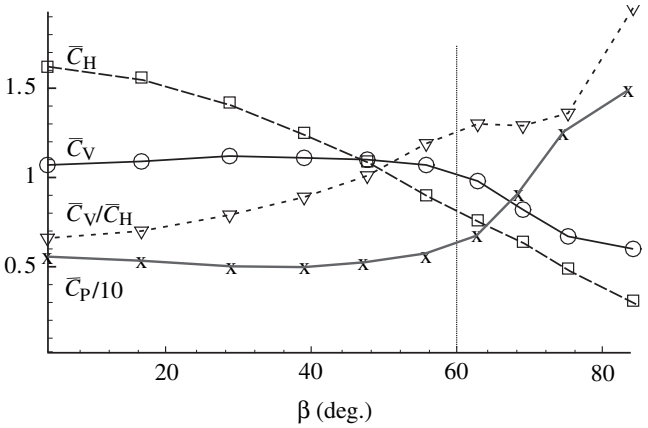

Fig. 5. Comparison of the averaged vertical ($\bar{C}_V$) and horizontal ($\bar{C}_H$) force coefficients and specific power ($\bar{C}_P$) as a function of β. $\bar{C}_P$ is scaled by a factor of 1/10 to fit in the graph.

An explanation of anomalously high lift coefficients obtained in previous estimates

Now I return to the question discussed in the Introduction about the high lift coefficients obtained in quasi-steady analysis of dragonflies (Weis-Fogh, 1973; Norberg, 1975; Ellington, 1984). The lift to drag ratio during downstroke was assumed to be ~6.5 (Weis-Fogh, 1973; Norberg, 1975), which is based on the value at small angle of attack in locust flight (Jensen, 1956). According to the current computation in the corresponding case of β=63°, the drag contributes about 76% of the net vertical force. Therefore, the assumption of a lift to drag ratio of 6.5 is equivalent to assuming a drag contribution of about (24/6.5)% of the vertical force. Consequently, it ignores about 72% [76–(24/6.5)] of the net vertical force. This would result in approximately a factor of four increase in the estimate of the lift coefficient. If we include the computed drag, Norberg's estimate (C_L≈3.5–6.1; Norberg, 1975) would yield a C_L of ~0.9–1.5, which is much more reasonable.

The role of drag in normal hovering

Dragonflies and hoverflies, which use a highly inclined stroke plane, are examples where ignoring drag can lead to obvious contradictions. One might ask to what degree drag is relevant in understanding normal hovering, which is employed by most insects including flies and bees. The wing tip of different insects typically traces out shapes of an oval, a parabola or a figure of eight, under different experimental conditions (tethered *vs* free flight; Marey, 1868; Hollick, 1940; Jensen, 1956; Nachtigall, 1974; Ellington, 1984; Zanker and Götz, 1990; Fry et al., 2003), but the aerodynamic consequences of these variations have not been much discussed.

Here, I suggest that a figure of eight, an oval or a parabola can all be decomposed into pairs of dragonfly-like strokes, as illustrated in Fig. 1C,D. The deviation from a horizontal stroke plane permits the insect to use some of the drag to support its weight during the plunging-down motion. Recent force measurements on a robotic wing mimicking hovering of fruitflies show that the upward force has a substantial component in the direction of drag (see fig. 3A in Fry et al., 2003). These new results, together with the analysis here, suggest that normal-hovering insects can also use part of drag to support their weight. Another implication is that the instantaneous orientation of the stroke plane is a relevant parameter when constructing model wing motions.

Improving efficiency by eliminating half of a stroke in normal hovering

The magnitude of drag in normal hovering considered here

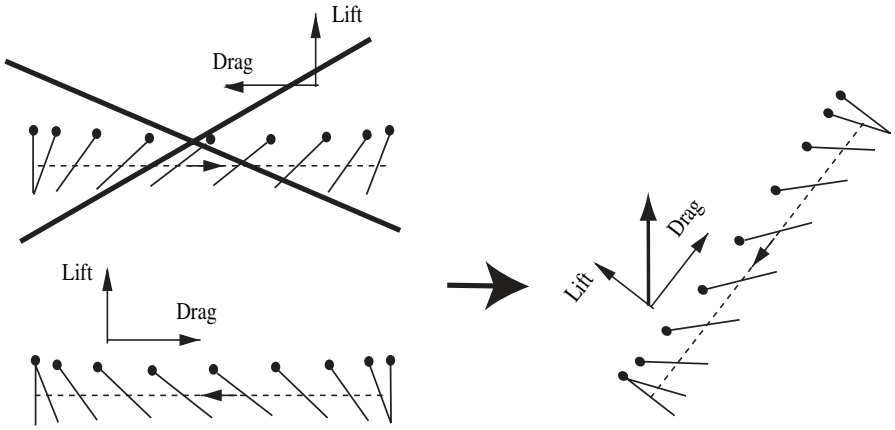

Fig. 6. Reducing specific power by eliminating half of a stroke.

(see Fig. 2A) is greater than that of lift (C_D=1.61 and C_L=1.07) yet, because of the use of strict horizontal stroke plane, the drag makes no contribution to the net force. Large drag was also found in simulations of a family of normal hovering (Wang et al., 2004), in particular near the wing reversal, and in an extensive experimental study of 191 hovering kinematics, where stroke amplitude, angle of attack, deviation of the stroke plane, and timing and duration of wing rotation were varied (Sane and Dickinson, 2001).

Here is a strategy to benefit from the large drag found in these symmetric strokes. Instead of using both half-strokes, take a half-stroke and make it a downstroke by tilting the stroke plane such that the net force points vertically up (Fig. 6). The upstroke simply returns to the starting position with a zero angle of attack, which generates a negligible amount of force but also consumes a negligible amount of power.

If one applies this procedure to the case of symmetric stroke (Fig. 2A), the downstroke has a net coefficient of $\sqrt{1.61^2+1.07^2}$=1.98. The stroke plane should be tilted by approximately $\tan^{-1}(1.61/1.07)\approx 56°$, so the net force points upward. Since the upstroke contributes almost no force, the averaged force coefficient in a complete stroke is 1.98/2=0.99. The total power is also reduced by a factor of two since the upstroke does almost no work. Comparing this new stroke with the symmetric one, the specific power (total power per supported weight) is reduced by a factor of (1/2)(1.07/0.99)=0.54. Similarly, one can apply the same procedure to the experimental case of α=50° and ϕ=180° in Sane and Dickinson (2001), where C_D=3.16 and C_L=1.87 and the net force coefficient during the downstroke is 3.67. The stroke plane should be tilted by ~63°. The average force in the new stroke is almost the same as in the original stroke, while the specific power over a period is reduced by a factor of two. In both cases, by eliminating half of the stroke, the wing supports about the same weight but consumes half of the power.

This conceptual example shows that a rowing-like motion can, in some cases, be more efficient than an airfoil-like motion, which is quite the opposite to what Weis-Fogh (1973) had anticipated.

Concluding remarks

I hope that the collection of lessons learned here helps to bring unsteady drag on an equal footing with unsteady lift in studies of flapping motions in fluids. This also suggests a need for developing better theories of predicting unsteady drag in separated flows (Pullin and Wang, 2004) and experiments and computations to examine the role of drag in the locomotion in fluids (Wang, 2005).

List of symbols

A_0	amplitude of translation
A_w	wing cross-sectional area
B	amplitude of rotation
c	chord
$\bar{C}_D$	averaged drag coefficient
C_D	drag coefficient
$\bar{C}_H$	averaged horizontal force coefficient
C_H	horizontal force coefficient
$\bar{C}_L$	averaged lift coefficient
C_L	lift coefficient
$\bar{C}_P$	averaged specific power
$\bar{C}_V$	averaged vertical force coefficient
C_V	vertical force coefficient
f	frequency
$F_D(t)$	drag
$\mathbf{F}_p$	pressure force
F_V	vertical force
$\mathbf{F}_v$	viscous force
$\bar{P}$	averaged power exerted by the wing to the fluid
p	pressure
$\mathbf{r}$	position relative to the wing center
Re	Reynolds number
$\mathbf{\Omega}$	rotational velocity of the wing
s	arc length
$\hat{s}$	tangent vector along the ellipse
S	scaling factor
t	time
$\mathbf{u}$	fluid velocity field
$\mathbf{U}_0$	translational velocity of the wing
$\mathbf{U}_{max}$	maximum translational velocity
α_A	angle of attack
$\alpha(t)$	chord orientation relative to the stroke plane
β	angle of inclination of the stroke plane
ϕ	phase delay between rotation and translation
ν	kinematic viscosity
ρ	air density
ω	vorticity field

I thank A. Andersen, S. Childress, M. Dickinson, R. Dudley, C. Ellington and P. Lissaman for useful feedback on an earlier version of this work (http://arxiv.org/ps/physics/0304069) and A. Ruina for helpful discussions. The work is supported by the AFOSR, NSF and Packard Foundation.

References

Blake, R. W. (1981). Mechanics of drag-based mechanism of propulsion in aquatic vertebrates. *Symp. Zool. Soc. Lond.* **48**, 29-52.

Childress, S. (1981). *Swimming and Flying in Nature*. Cambridge: Cambridge University Press.

Dickinson, M. H. (1996). Unsteady mechanisms of force generations in aquatic and aerial locomotion. *Am. Zool.* **36**, 537-554.

Dickinson, M. H. and Götz, K. G. (1993). Unsteady aerodynamic performance of model wings at low Reynolds numbers. *J. Exp. Biol.* **174**, 45-64.

Dickinson, M. H., Lehmann, F. O. and Sane, S. P. (1999). Wing rotation and the aerodynamic basis of insect flight. *Science* **284**, 1954-1960.

E, W. and Liu, J. (1996). Essentially compact schemes for unsteady viscous incompressible flows. *J. Comp. Phys.* **126**, 122-138.

Ellington, C. P. (1984). The aerodynamics of hovering insect flight I–V. *Phil. Trans. R. Soc. Lond.* B **305**, 1-181.

Ellington, C. P., van den Berg, C., Willmott, A. P. and Thomas, A. L. R. (1996). Leading-edge vortices in insect flight. *Nature* **384**, 626-630.

Freymuth, P., Gustafson, K. and Leben, R. (1991). Visualization and

computation of hovering mode. In *Vortex Method and Vortex Motion* (ed. K. Gustavson and J. Sethian), pp. 143-169. Philadelphia: Society for Industrial and Applied Mathematics (SIAM).

Fry, S. N., Sayaman, R. and Dickinson, M. H. (2003). The aerodynamics of free-flight maneuvers in *Drosophila*. *Science* **300**, 495-498.

Gustafson, K., Leben, R. and McArthur, J. (1992). Lift and thrust generation by an airfoil in hover modes. *Comp. Fluid Dynamics J.* **1**, 47.

Hollick, F. S. J. (1940). The flight of the dipterous fly *Muscina stabulans* Fallen. *Phil. Trans. R. Soc. B*, **230**, 357-390.

Horridge, G. A. (1956). The flight of very small insects. *Nature* **178**, 1334-1335.

Jensen, M. (1956). Biology and physics of locust flight. III. The aerodynamics of locust flight. *Proc. Roy. Soc. Lond. B* **239**, 511-551.

Leishman, J. (2000). *Principles of Helicopter Aerodynamics*. Cambridge: University of Cambridge.

Marey, E. J. (1868). Determination experimentale du mouvement des ailes des insectes pendant le vol. *C. R. Acad. Sci. Paris* **67**, 1341-1345.

Nachtigall, W. (1974). *Insects in Flight*. New York: McGraw–Hill.

Norberg, R. A. (1975). Hovering flight of the dragonfly *Aeschna juncea*: kinematics and aerodynamics. In *Swimming and Flying in Nature*, vol. 2 (ed. T. Y. Wu, C. J. Brokaw and C. Brennen), pp. 763-780. New York: Plenum Press.

Pullin, D. I. and Wang, Z. J. (2004). Unsteady forces on an accelerating plate and application to hovering insect flight. *J. Fluid Mech*. **509**, 1-21.

Purcell, E. M. (1977). Life at low Reynolds number. *Am. J. Phys.* **45**, 3-11.

Sane, S. and Dickinson, M. H. (2001). The control of flight force by a flapping wing: lift and drag production. *J. Exp. Biol.* **204**, 2607-2626.

Sane, S. and Dickinson, M. H. (2002). The aerodynamic effects of wing rotation and a revised quasi-steady model of flapping flight. *J. Exp. Biol.* **205**, 1087-1096.

Taylor, G. I. (1985). *Low Reynolds Number Flows* (video recording). Chicago: Encyclopaedia Britannica Educational Corp.

Vogel, S. (1996). *Life in Moving Fluids*. Princeton, NJ: Princeton University.

von Holst, E. and Kuchemann, D. (1941). Biological and aerodynamical problems of animal flight. *Naturwissenschaften* **46**, 39-58.

Wakeling, J. M. and Ellington, C. P. (1997). Dragonfly flight II: velocities, accelerations and kinematics of flapping flight. *J. Exp. Biol.* **200**, 557-582.

Wang, Z. J. (2000a). Two dimensional mechanism of hovering. *Phys. Rev. Lett.* **85**, 2216-2219.

Wang, Z. J. (2000b). Vortex shedding and frequency selection in flapping flight. *J. Fluid Mech.* **410**, 323-341.

Wang, Z. J. (2005). Dissecting insect flight. *Annu. Rev. Fluid. Mech.* **37**, 183-210.

Wang, Z. J., Birch, J. and Dickinson, M. H. (2004). Unsteady forces and flows in low Reynolds number hovering flight: two-dimensional computations *vs* robotic wing experiments. *J. Exp. Biol.* **207**, 449-460.

Weis-Fogh, T. (1973). Quick estimates of flight fitness in hovering animals, including novel mechanisms for lift production. *J. Exp Biol.* **59**, 169-230.

Wu, T. Y.-T., Brokaw, C. J. and Brennen, C. (1975). *Swimming and Flying in Nature*, vol. I and vol. II. New York, London: Plenum Press.

Zanker, J. M. and Götz, K. G. (1990). The wing beat of *Drosophila melanogaster* II. dynamics. *Phil. Trans. R. Soc Lond. B* **327**, 19-44.